

CRITICAL LENGTH MEASUREMENTS IN CARBON FIBRES DURING SINGLE FIBRE FRAGMENTATION TESTS USING ACOUSTIC EMISSION

Carlo Santulli

University of Reading, School of Construction Management and Engineering

Whiteknights, Reading RG6 6AY

The single fibre fragmentation test (SFFT) is a well-known experimental test, which allows the study of fibre failure in its simplest form [1-2]. The principle is that a single fibre embedded in a matrix repeatedly breaks until all fragment lengths are within a critical distance. Once the fibre has broken for the first time, successive breakage happens in regions removed from the initial failure, often referred to as *polled areas* [3]. Acoustic emission (AE) has been extensively used for the detection and localisation of fibre breakage during SFFT tests, in carbon [4-5], Kevlar [6-7] and glass fibre composites [8-9]. In all cases, in spite of the small diameter of the fibres, nearly all fibre breakages appeared to have been detected and associated with a single acoustic emission event, an occurrence that has been defined as *one-to-one correspondence* [10]. Moreover, the number of acoustic emission events detected corresponded with considerable accuracy with the fibre breakages observed by other methods e.g., optical microscopy [11]. This allowed the determination of Weibull statistical strength parameters for the fibres based on the number of acoustic emission hits detected [12]. From the above parameters and the average length of fibre fragment, the interfacial strength can be determined, assuming that the fibres are constant in diameter, which is acceptable for glass and carbon fibres, much less so for brittle e.g., ceramic, monofilaments [13].

When dealing with localisation of acoustic emission events, a considerable number of issues arise. Ideally, in an environment with sufficient signal to noise ratio, two sensors can be

calibrated for localisation, using at every location the correct value for wave velocity, which may vary up to 10% with the applied stress [14]. If this is the case, differences in wave arrival time at the sensors of less than a microsecond can be measured, so that AE events can be localised with accuracy in the order of 0.1 mm. This can be achieved by most recent acoustic emission systems by placing the sensors at a mutual separation distance not exceeding 30-40 mm, therefore compatible with the most common gauge lengths applied in SFFT tests.

In this work, a single T300 high strength carbon fibre filament (7 μm . diameter) was embedded in three different polymeric matrices (polycarbonate, polyurethane and epoxy). A total number of fifteen dog-bone specimens, five per matrix, were prepared, each with total length 45 mm. Tests were performed in displacement control mode with a crosshead speed equal to 0.13 mm/min. During these tests, acoustic emission was continuously monitored using pairs of piezoelectric microsensors (5 mm. diameter), resonant at 300 kHz, placed at a mutual distance centre-to-centre of 30 mm, each 15 mm from the middle of the sample. AE data were treated using a PAC Mistras 2000 system. Only single burst signals have been considered, triggering the two channels i.e., yielding an AE event in an interval of less than 11.5 μs , corresponding to the time at which the 30 mm distance between the sensors is covered at the wave speed, measured along the carbon fibre, of 2600 m/s.

The strain measured on the fibres during SFFT tests was 1.02(\pm 0.20)%. A number of conditions need to be verified in order for the test to be valid for critical fibre length and Weibull statistical measurements. These include fibre and matrix both behaving linearly and elastically during fragmentation, fibre-matrix adhesion being sufficiently strong, so that no pullout occurs [15], and the interface being of the same thickness across the composite [16]. It has been recently observed that the performance of SFFT tests at higher strain rates, in place of giving shorter fibre fragments as the major effect, induces a larger occurrence of creep, so that the test is no longer valid for fracture mechanics purposes [17].

The low strain rate adopted resulted in a linear elastic behaviour of fibres and matrix, although in some cases fibre-matrix adhesion was not as strong as expected, and this gave rise to early pullout of the fibres, even if no significant torsion of the samples was observed. As a consequence, results from the specimens showing early pullout were not considered for analysis. Weibull parameters measurements can still be fairly accurate, since their values were shown, as reported below, not to change very much with the polymer used as matrix in the SFFT samples. However, fragment length distribution may differ considerably, being less or more scattered, as can be observed by comparing Figure 1a, for a polycarbonate specimen, with Figure 1b, for a polyurethane specimen.

Acoustic emission counts of the signals associated with fibre breakages (Figure 2a) appear to be only slightly affected by the position of the fibre: to work out a possible trend, further testing would be needed. Even more dubious appears the relation of AE energy, expressed in units representing the envelope area under the signal, with the level of strain on the fibre (Figure 2b). This indicates that the measured acoustic energy does not exactly represent the stored elastic energy in the segment at failure, because in the latter case it should be proportional to the stress on the fibre [18].

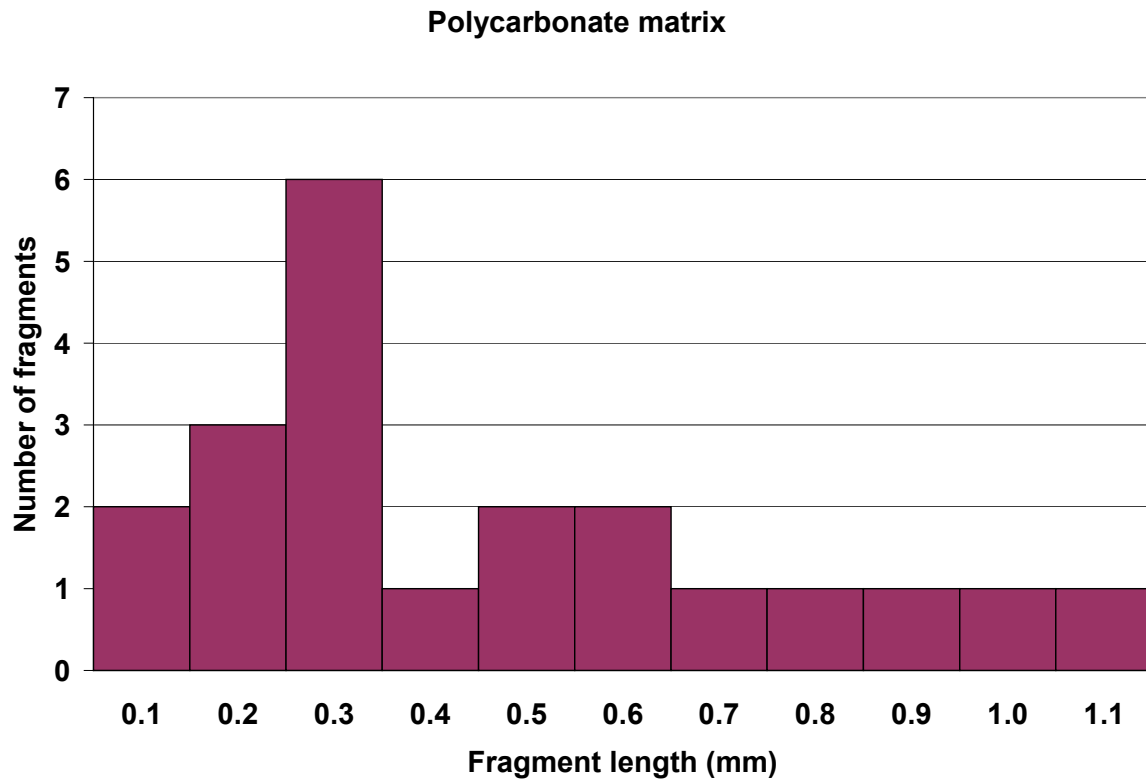


Figure 1a Length distribution of T300 fibre fragments in a polycarbonate matrix

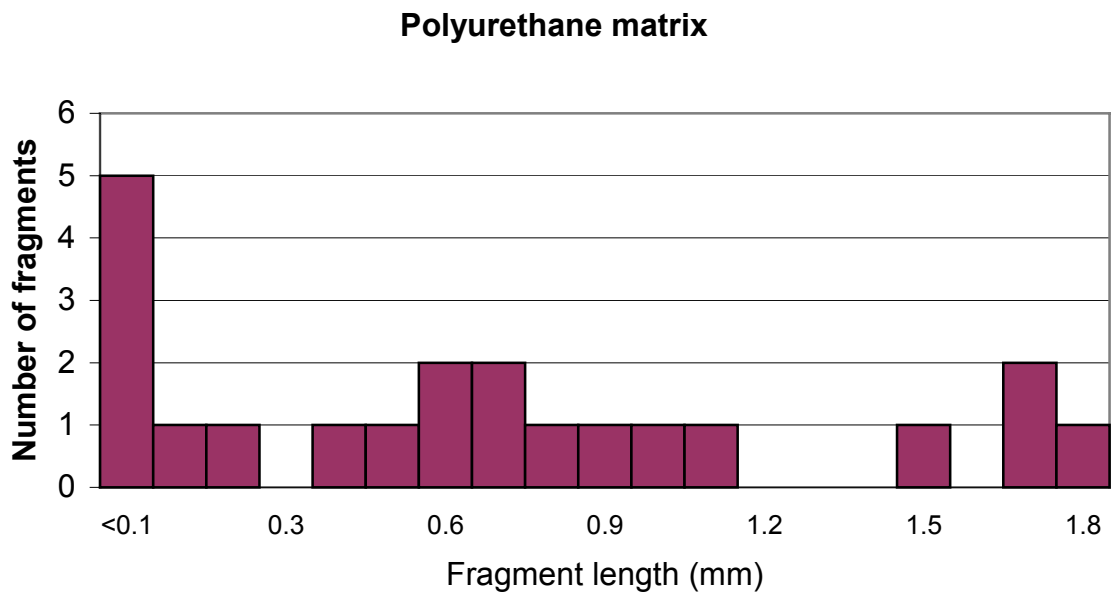


Figure 1b Length distribution of T300 fibre fragments in a polyurethane matrix

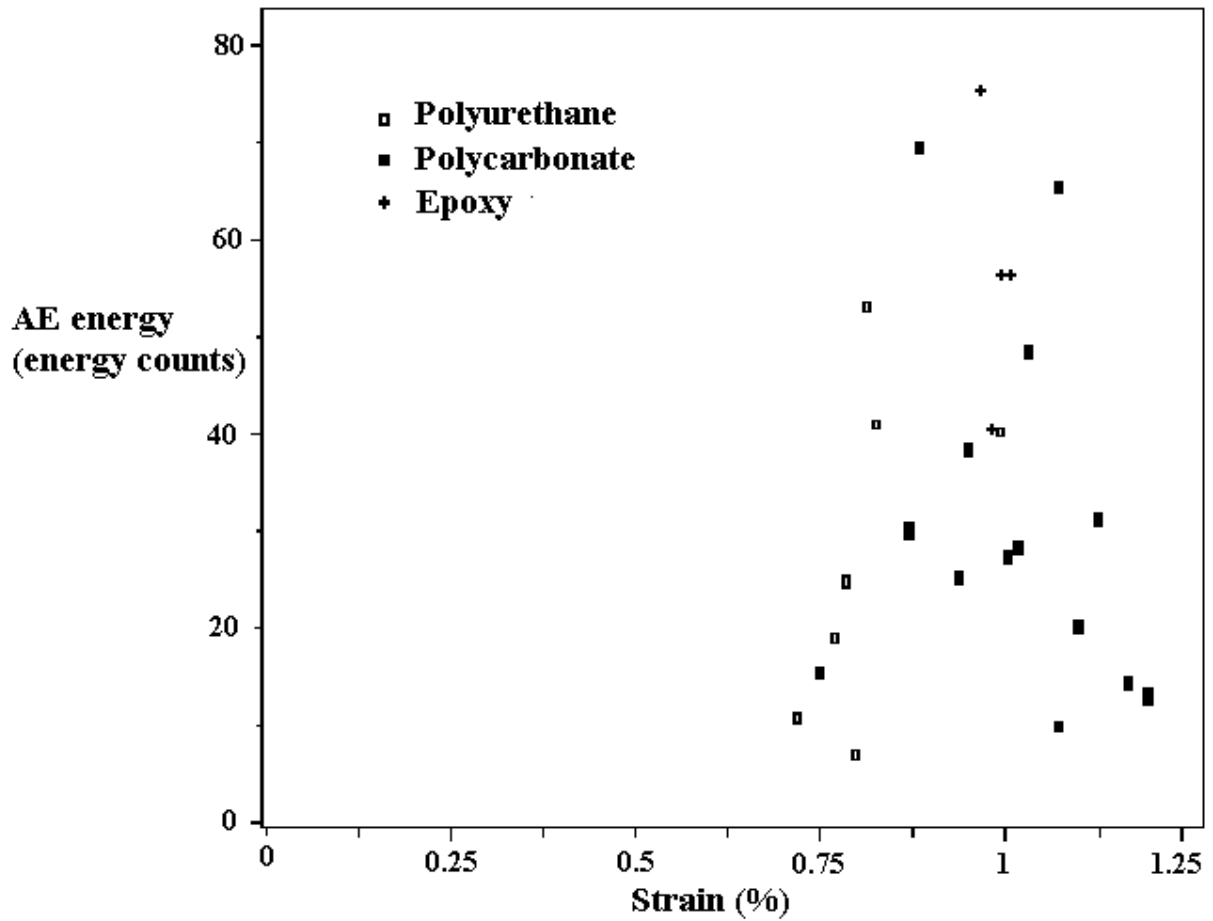


Figure 2a Energies of acoustic emission events in three SFFT samples, one per matrix

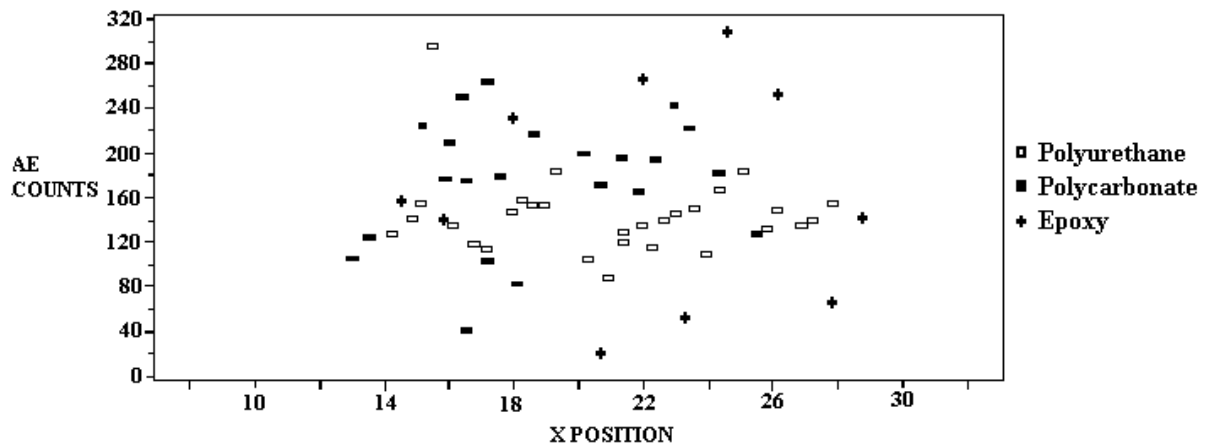


Figure 2b Counts of acoustic emission events in three SFFT samples, one per matrix

Analysing according to a two-parameters Weibull distribution, a number of approaches have been developed to predict the critical fibre length from measurements of fibre fragment length obtained using acoustic emission. The theory developed in [19] was adopted, that,

neglecting the effect of fibre ends shielding possible flaw sites from fracture, as is possible in a low stress region, gives for the number of fibre breaks N over a gauge length L_o this simple power law:

$$N(L_o) = \left(\frac{\sigma_f}{\alpha_o} \right)^\beta \quad (1)$$

where σ_f is fibre stress and α_o and β are size and shape parameters. Since in this work, strain ϵ_a is measured in place of stress, and from the former, stress σ_f is obtained as $\sigma_f = \epsilon_a E_f$,

In this way Eq. (1) can be written as $\ln N = \beta \ln \epsilon_a E_f - \beta \ln \alpha_o$, so that β can be determined from the slope of the $\ln N$ vs. ϵ_a , and α_o from its intercept at $\ln N = 0$, as suggested in [11]. Typical curves obtained for the three matrices are represented in Figure 3. The difference in slope observed between the initial and the following part of the curve has to be ascribed to the combination of two effects, the initial irregularities in loading behaviour and the occurrence of creep after the fibre underwent the first few failures [11]. The presence of both effects would rather suggest considering a linear regression of the whole curve than excluding a part of it. The inaccuracy of this measurement can be reduced with the alternative method described below.

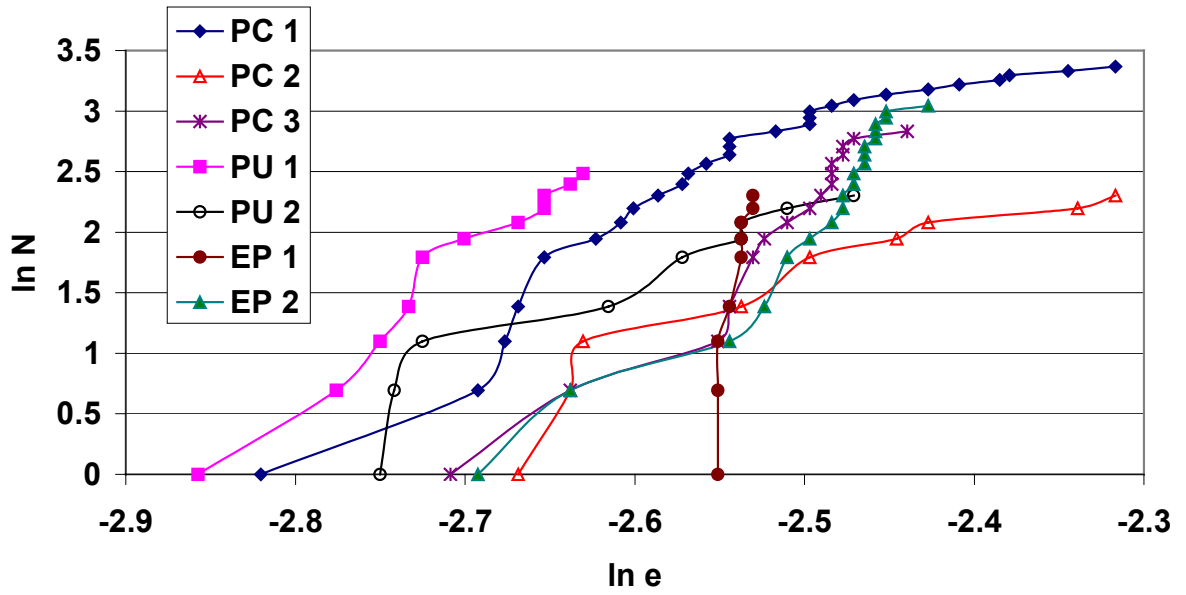


Figure 3 Typical curves obtained from acoustic emission study of fibre fragmentation
(N= number of fibre breakages)

In place of considering $N(L_o)$, α_o and β can be determined using the mean fibre fragment length $l(\sigma)$, obtained from acoustic emission localisation:

$$l(\sigma) = \left(\frac{\sigma}{\alpha_o} \right)^\beta \quad (2)$$

Hence, adopting the suggestion from [20] over the Kelly-Tyson [15] expression for maximum critical fibre length l_c , that the actual fragment lengths vary from $0.5 l_c$ to l_c , so that, assuming a Gaussian distribution, the mean fragment length l is $0.75 l_c$, the interfacial yield stress can be obtained from:

$$\tau = \frac{d\sigma_f}{2\ell} 0.75 \quad (3)$$

The values obtained from acoustic emission localisation for α_o , β , $l(\sigma)$ and τ using Eq. 1-3 are reported in Table 1.

Sample	α	β	L_{av} (mm)	ϵ_{max} (%)	τ (MPa)
PC 1	13590	6.87	0.44	0.986	13.9
PC 2	15800	5.58	1.54	0.883	3.4
PU 1	13100	11.23	0.61	0.720	7.1
PU 2	14580	6.89	0.48	0.845	10.5
EP 1	15190	12.25	0.47	0.872	11.1
EP 2	16300	11.66	1.37	0.883	3.9

Table 1 Values obtained for Weibull parameters,

average fragment length, interface stress and strain at failure

Comments on the results obtained should refer first to the fact that, as previously observed [14], the matrix has very little effect on the values of Weibull parameters: however, in these tests they appear to be substantially lower than those measured for T300 fibres in [10]. This should rather be ascribed to the experimental set-up adopted for tensile tests, which was not able to completely rule out a slight torsion of the samples. Less important appeared to be the limitation of obtaining fibre stress from an indirect measurement of strain, because the effect of matrix cracks or pullout on stress-strain linearity has been shown to be negligible for high strength carbon fibres [21]. In addition, the accuracy of acoustic emission prediction of Weibull values was observed to grow with the number of breakages in each fibre [22]. In these tests, although a visual one-to-one correspondence between acoustic emission events and fibre breaks was observed, the number of fibre breakages was probably not high enough to offer a good level of accuracy. In spite of this, the evolution of acoustic emission technique leading to more accurate systems, involving a measurement of real fracture energy during the tests, may allow integration of Weibull parameter results with other information on the single

fibre breakage. This would ultimately contribute to a fuller understanding of the process of fibre fragmentation and to the local measurement of stresses at fibre-matrix interface.

REFERENCES

1. Curtin WA, *Appl. Phys. Lett.* **58**, 1991, 1155-1157.
2. Feillard P, Désarmot G, Favre JP, *Compos. Sci. Technol.* **50**, 1994, 265-279.
3. Westbury MC, Drzal LT, *J. Compos. Technol. Res.* **13**, 1991, 22-28.
4. Desaegeer M, Wevers M, Verpoest I, AECM 4 Conference, Seattle, July 1991.
5. Rouby D, Favre JP, 16th Annual Meeting EWGAE, London, Sept. 1986.
6. Ma BT, Schadler LS, Laird C, Figueroa JC, *Polym. Compos.* **11**, 1990, 211-216.
7. Netravali AN, Sachse W, *Polym. Compos.* **12**, 1991, 370-373.
8. Narisawa I, Oba H, *J. Mater. Sci.* **19**, 1984, 1777-1786.
9. Park JM, Subramanian RV, *J. Adhes. Sci. Technol.* **8**, 1994, 133-150.
10. Ni QQ, Jinen E, *Eng. Fract. Mech.* **56**, 1997, 779-796.
11. Clough RB, McDonough WG, *Compos. Sci. Technol.* **56**, 1996, 1119-1127.
12. Andersons J, Tamusz V, *Compos. Sci. Technol.* **48**, 1993, 57-63.
13. Morimoto T, *Compos. Part A- Appl. S.* **34**, 2003, 597-601
14. Netravali AN, Topoleski LT, Sachse WH, Phoenix SL, *Compos. Sci. Technol.* **35**, 1989, 13-19.
15. Kelly A, Tyson WR, *J. Mech. Phys. Solids* **13**, 1965, 329.
16. Hayes SA, *Compos. Part A- Appl. S.* **32**, 2001, 379-389
17. Gong XJ, Arthur JA, Penn LS, *Polym. Compos.* **22**, 2001, 349-360.
18. Arridge RGC, *Mater. Sci. Technol.* **3**, 1987, 609-615.
19. Gulino R, Phoenix SL, *J. Mater. Sci.* **26**, 1991, 3107-3118.
20. Wimolkiatisak AS, Bell JP, *Polym. Compos.* **11**, 1990, 274-279.
21. Netravali AN, Li ZF, Sachse W, Wu HF, *J. Mater. Sci.* **26**, 1991, 6631-6638.
22. Manor A, Clough RB, *Compos. Sci. Technol.* **45**, 1992, 73-81.